

Intersublevel polaron dephasing in self-assembled quantum dots

E. A. Zibik,¹ T. Grange,² B. A. Carpenter,¹ R. Ferreira,² G. Bastard,² N. Q. Vinh,³ P. J. Phillips,³ M. J. Steer,⁴ M. Hopkinson,⁴ J. W. Cockburn,¹ M. S. Skolnick,¹ and L. R. Wilson¹

¹*Department of Physics and Astronomy, University of Sheffield, Sheffield S3 7RH, United Kingdom*

²*Laboratoire Pierre Aigrain, Ecole Normale Supérieure, 24 rue Lhomond, 75231 Paris Cedex 05, France*

³*FOM Institute Rijnhuizen, PO Box 1207, NL-3430 BE, Nieuwegein, The Netherlands*

⁴*EPSRC National Centre for III-V Technologies, Sheffield S1 3JD, United Kingdom*

(Received 12 November 2007; published 28 January 2008)

Polaron dephasing processes are investigated in InAs/GaAs dots using far-infrared transient four wave mixing (FWM) spectroscopy. We observe an oscillatory behavior in the FWM signal shortly (<5 ps) after resonant excitation of the lowest energy conduction band transition due to coherent acoustic phonon generation. The subsequent single exponential decay yields long intraband dephasing times of 90 ps. We find good agreement between our measured and calculated FWM dynamics, and show that both real and virtual acoustic phonon processes are necessary to explain the temperature dependence of the polarization decay.

DOI: [10.1103/PhysRevB.77.041307](https://doi.org/10.1103/PhysRevB.77.041307)

PACS number(s): 78.67.Hc, 42.50.Md, 71.38.-k, 78.47.-p

The strong spatial confinement of carriers in semiconductor quantum dots (QDs) leads to striking differences in the carrier-phonon interaction compared with systems of higher dimensionality. In particular, the discrete energy level structure in QDs results in long exciton and electron dephasing times,¹⁻⁴ making these semiconductor nanostructures highly attractive for implementation in quantum information processing applications. The study of dephasing mechanisms in QDs is commonly carried out using transient four wave mixing (FWM) spectroscopy. Using resonant interband excitation, FWM measurements have revealed the absorption line shape of single QDs to consist of a narrow zero phonon line (ZPL) and an acoustic phonon-related broadband centered at the same energy. The only intraband FWM study⁵ involved resonant excitation of high energy transitions in the valence band of *p*-doped QDs yielding dephasing times ~ 15 ps. However, it was not possible to determine the dephasing mechanisms in this case.

Intraband studies of the well-resolved lowest energy conduction band electron transitions in InAs/GaAs QDs have provided deep insight into the electron-phonon interaction and carrier relaxation processes in *n*-doped samples. Clear evidence of strong coupling between electrons and phonons, resulting in polaron formation, has been demonstrated using magnetotransmission measurements.⁶ Ultrafast studies^{7,8} of polaron decay have shown that the previously assumed “phonon bottleneck” picture is not valid. Compared with semiconductor quantum wells, the intraband population relaxation time in QDs is long (≈ 50 ps) suggesting relatively long dephasing times. However, there have been no reports of direct dephasing measurements to date.

In the present Rapid Communication we present investigations of intraband dephasing in *n*-doped QDs using degenerate FWM. Our calculations of the absorption line shape in this case show marked differences in comparison with the interband absorption.⁹ The intraband line shape consists of peaked acoustic phonon sidebands separated by ~ 1.5 meV from the ZPL, which corresponds to phonons with wavelength close to the dot size, and is reminiscent of the line shape associated with impurity-bound electron transitions.¹⁰

Using pulse durations short enough to excite both the ZPL and acoustic phonon sidebands we find damped oscillations in the FWM signal, indicative of coherent acoustic phonon generation, followed by a single exponential decay. At low temperature, we have measured an intersublevel dephasing time of $T_2 \approx 90$ ps. This time is approximately 2 orders of magnitude longer than typical dephasing times in higher dimensional (quantum well) systems.¹¹ The relatively long intraband dephasing time in QDs is key to the efficient operation of new types of mid-infrared QD-based devices, such as intersublevel polaron lasers¹² and may be relevant for potential device applications such as qubits for quantum information processors.¹³

The investigated samples were grown on (100) GaAs substrates by molecular beam epitaxy in the Stranski-Krastranow mode. They comprise 80 layers of InAs self-assembled QDs separated by 50-nm-wide GaAs barriers, thus preventing both structural and electronic coupling between QD layers. The polaron transitions were studied between *s*-like ground (*s*) and *p*-like first excited (*p*) states within the conduction band. To populate the *s* state, the samples were δ -doped with Si 2 nm below each QD layer. The doping density was controlled in such a way that the average doping did not exceed one electron per dot (see Ref. 14 for more details). Absorption spectra of the investigated QD samples were studied elsewhere.⁸ Since our QD samples contain ~ 1 *e*/dot only the ground state is occupied and therefore the incident radiation polarized along either the $[0\bar{1}1]$ or $[011]$ crystallographic directions excites a transition from the *s* state to either the lower (p_x) or higher (p_y) energy laterally confined state. The absorption peaks associated with these transitions are inhomogeneously broadened by ~ 5 meV due to the QD size and composition distribution. The $\Delta_{pp} \approx 5$ meV anisotropy splitting between the two peaks can be explained by QD asymmetry due to piezoelectric field effects^{15,16} and the atomistic symmetry.¹⁷

We studied the coherent polaron polarizations in QDs using a standard two-pulse photon echo arrangement in a non-collinear geometry.¹⁸ The far-infrared time-integrated FWM measurements were carried out using the Dutch free electron

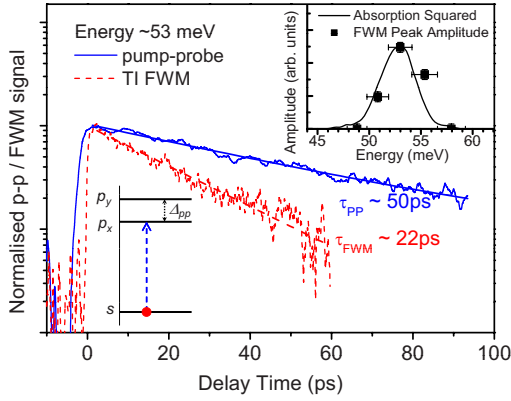


FIG. 1. (Color online) Comparison of time integrated FWM (dashed line) and pump-probe (solid line) signals measured at 10 K and transition energy of ~ 53 meV as a function of the delay time between the incoming pulses. The inset exhibits the absorption squared and FWM signal intensity at peak maximum vs the transition energy for the same sample. Also shown is the schematic diagram of the polaron energy structure in InAs QDs.

laser (FELIX) which provides subpicosecond, tuneable laser pulses. We used a ratio of 1:2 between the two incoming pulses with wave vectors \mathbf{k}_1 and \mathbf{k}_2 , and the intensity of the third order nonlinear signal was measured in the $2\mathbf{k}_2 - \mathbf{k}_1$ direction. The applied peak power density was ~ 50 W/mm².¹⁹ The measurements were performed in the $\chi^{(3)}$ regime, where the intensity of the FWM signal has a cubic dependence on the excitation intensity.

The comparison between the FWM signal and the pump-probe signal at the same s - p_x transition energy of 53 meV is shown in Fig. 1. To verify that the FWM signal arises from excitation in resonance with the s - p_x transition in the QDs we measured the spectral dependence of the FWM signal amplitude and find a good correspondence with the square of the linear s - p_x absorption signal (inset Fig. 1).

Unlike pump-probe, the FWM signal is sensitive not only to changes in carrier population but also to a decay of coherent optical polarizations, thus providing a direct measurement of the excited carrier dephasing time. The decay time of the FWM signal is fitted with a single exponential curve yielding $\tau_{FWM} \approx 22$ ps. In the case of inhomogeneously broadened transitions the dephasing time is $T_2 = 4\tau_{FWM}$,²⁰ and thus the low temperature dephasing time of the s - p_x transition is $T_2 \approx 88$ ps. This is close to the value $2T_1 \approx 100$ ps deduced from independent pump-probe measurements. The homogenous linewidth $\Gamma_2 = 2\hbar/T_2$ can be decomposed as the sum of population relaxation $\Gamma_1 = \hbar/T_1$ and pure dephasing $\Gamma_2^* = 2\hbar/T_2^*$ contributions.²² The relation $T_2 \approx 2T_1$ indicates that pure dephasing processes are negligible at low temperature.

We find that at low temperature the polaron dephasing time decreases from $T_2 \approx 88$ ps at an excitation energy $\hbar\omega \approx 53$ meV to $T_2 \approx 60$ ps at $\hbar\omega \approx 48$ meV.²³ This is consistent with the energy dependence of the polaron decay time T_1 ,^{8,21} which decreases as the polaron energy approaches that of the LO phonon. As we have shown in Ref. 8, the polaron relaxation to the ground state is due to anharmonic disintegration of polarons into two high energy acoustic

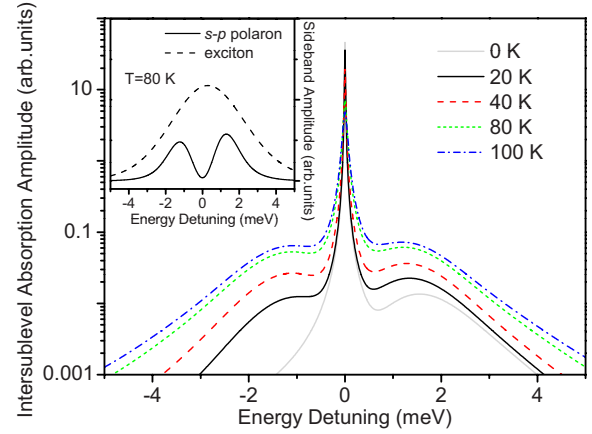


FIG. 2. (Color online) Calculated InAs single-dot polaron absorption at different temperatures. The ZPL transition energy is taken as zero energy. Inset shows the comparison between the acoustic phonon sidebands for intersublevel polaron (solid line) and ground state exciton (dashed line) at $T=80$ K. The ZPL is not considered for clarity.

phonons, leading to the following temperature dependence: $\Gamma_1 = [1 + N(\hbar\omega_p/2)]^2 \hbar/T_1^0$, where $N(\hbar\omega) = 1/(e^{\hbar\omega/k_B T} - 1)$ is the Bose occupation number, T_1^0 is the polaron lifetime at low temperature, and $\hbar\omega_p$ is the s to p_x energy transition. But as we shall see below, $\Gamma_2 \gg \Gamma_1$ when the temperature is increased, indicating that pure dephasing processes become dominant.

In order to take into account additional sources of dephasing, we consider the polaron interaction with bulklike longitudinal acoustic (LA) phonon modes:

$$V = \sum_{i,j} \sum_q M_q^{ij} (a_q + a_{-q}^\dagger) |i\rangle \langle j| \quad (1)$$

where $M_q^{ij} = D_c \sqrt{\frac{\hbar q}{2\rho c_s V}} \langle i | e^{iq \cdot r} | j \rangle$ and $|i\rangle$ denotes the polaron state with the dominant component of the electron wave function $i = s, p_x$ or p_y . The deformation potential constant for the conduction band is taken as $D_c = -7.2$ eV,²⁴ the sound velocity is $c_s = 5000$ m s⁻¹ and the density $\rho = 5.32$ g cm⁻³. The diagonal parts within the polaron basis ($i=j$) are treated within the independent Boson model,²⁵ and results in phonon sidebands as replicas to the ZPL. The lineshape of the absorption as a function of the energy detuning ε is then given by $A(\varepsilon) = Z e^f(\varepsilon)$, where the exponential part is taken in the convolution sense ($e^f = \delta + f + f \otimes f/2 + \dots$) of the function:

$$f(\varepsilon) = \sum_q \frac{|M_q^{p_x p_x} - M_q^{s s}|^2}{\varepsilon^2} [N(|\varepsilon|) + \Theta(\varepsilon)] \delta(|\varepsilon| - \hbar\omega_q), \quad (2)$$

where Θ is the Heaviside function. The weight of the ZPL is given by $Z = \exp[-\int_{-\infty}^{+\infty} d\varepsilon f(\varepsilon)]$. Calculation of $A(\varepsilon)$, convolved with a Lorentzian of linewidth Γ_2 as calculated below, is shown in Fig. 2 for different temperatures. Due to cancellations of the contributions from s and p levels for long wavelength phonons in Eq. (2), $f(\varepsilon)$ behaves as ε^4 close to zero detuning $\varepsilon=0$ and is peaked around 1.5 meV, which corresponds to phonons with wavelength of about the dot size.²⁶ As a consequence, instead of a broad peak at the op-

tical transition energy as in the interband case, this leads to the appearance of two peaks separated from the ZPL in the absorption spectrum (see inset of Fig. 2).

As the ZPL is given by a delta function in Eq. (2), the diagonal parts of the phonon coupling do not contribute to the linewidth Γ_2 . On the other hand, off-diagonal acoustic phonon coupling between the close-in-energy p_x and p_y states are expected to contribute to pure dephasing processes. Taking into account these off-diagonal interactions with acoustic phonons up to two phonon processes,²⁷ we have calculated analytically the broadening associated with real and virtual transitions from the p_x state to the p_y state:²⁸

$$\Gamma_2^* = \frac{1}{2\pi} \int_0^{+\infty} d\varepsilon \frac{4\Delta_{pp}^2}{(\varepsilon + \Delta_{pp})^2} \times \frac{\Gamma_{pp}^2(\varepsilon)N(\varepsilon)[N(\varepsilon) + 1]}{(\varepsilon - \Delta_{pp})^2 + \left(\frac{\Gamma_{pp}(\varepsilon)[N(\varepsilon) + 1]}{2}\right)^2}, \quad (3)$$

where $\Gamma_{pp}(\varepsilon) = 2\pi \sum_q |M_q^{p_x p_y}|^2 \delta(\varepsilon - \hbar\omega_q)$. The integration of Γ_2^* around $\varepsilon = \Delta_{pp}$ corresponds to the linewidth $N(\Delta_{pp})\Gamma_{pp}(\Delta_{pp})$ of the real transition from p_x toward p_y by absorption of acoustic phonons, while phonons with an energy which is not in resonance with Δ_{pp} are responsible for virtual transitions, i.e., simultaneous absorption and emission of phonons of same energies but different wave vectors. By analyzing Eq. (3) we found that phonons which contribute mainly to these virtual transitions have energies ε between 2 and 3 meV, and their contribution to the dephasing is proportionnal to $N(\varepsilon)[N(\varepsilon) + 1]$. Therefore the full width at half maximum of the single dot homogeneous line $\Gamma_2 = \Gamma_1 + \Gamma_2^*$ has a strong temperature dependence.

We have calculated the FWM dynamics for excitation in resonance with the s to p_x transition, taking into account polaron decay to the s state, real and virtual transitions to the p_y state, as well as the presence of phonon sidebands.²⁹ The intensity of the FWM response to a δ pulse as a function of the delay time between the two pulse reads

$$I(t) \propto \Theta(t) \exp \left[-2\Gamma_2 t - 16 \int_{-\infty}^{+\infty} d\varepsilon f(\varepsilon) \sin^2 \left(\frac{\varepsilon t}{2\hbar} \right) \right]. \quad (4)$$

Experimental results measured at 53 meV and calculations of the FWM are presented in Fig. 3. Our calculations reveal the occurrence of decoherence oscillations between 0 and 5 ps due to the presence of acoustic phonon sidebands [see Fig. 3(a)], followed by an exponential decay of the FWM signal on a tens of picosecond time scale ($T_2/4$) due to real and virtual polaron transitions. The period of these oscillations is given approximatively by \hbar/ε_1 where $\varepsilon_1 \approx 1.5$ meV is the energy separation between the ZPL and the sideband peaks in Fig. 2. These oscillations, also observed experimentally [Fig. 3(b)], become more prominent with increasing temperature since the population of the acoustic phonons increases. In order to make a comparison with our experimental data, $I(t)$ is convolved by a 1.5-ps-long Gaussian pulse [see inset of Fig. 3(b)]. As the width of the sideband peaks is also in the ~ 1 -meV energy range, the damping of the oscillations occur on the same time scale as the oscillation, giving only one oscillation. Thus similar to exciton dephasing, the phonon sidebands are responsible for a fast nonexponential FWM decay on a picosecond time scale after excitation.³⁰

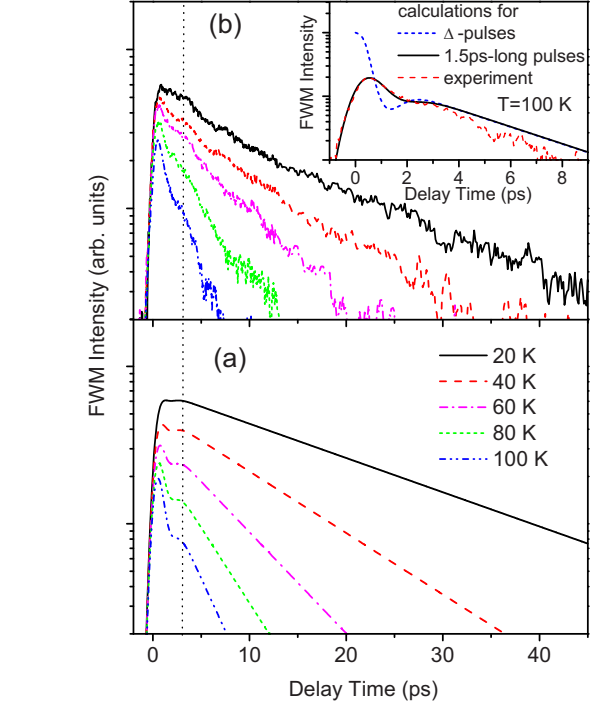


FIG. 3. (Color online) Temperature dependent four wave mixing signals: simulations (a) and experiment (b). Inset: calculated FWM curves at 100 K for δ pulses (dotted line) and 1.5-ps-long pulses compared with experimental data.

lations occur on the same time scale as the oscillation, giving only one oscillation. Thus similar to exciton dephasing, the phonon sidebands are responsible for a fast nonexponential FWM decay on a picosecond time scale after excitation.³⁰

The decay time of the exponential contribution to the FWM signal reduces significantly with increasing temperature from ≈ 22 ps at 10 K to ≈ 3 ps at 100 K, resulting in a decrease of the polaron dephasing time from ≈ 88 ps to ≈ 12 ps over the same temperature range. In Fig. 4, we have plotted the calculated total linewidth of ZPL $\Gamma_2 = \Gamma_1 + \Gamma_2^*$ (solid line), which shows very good agreement with the ex-

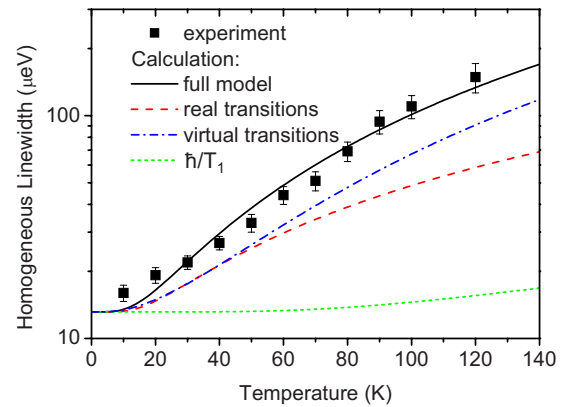


FIG. 4. (Color online) Temperature dependence of the polaron linewidth: experiment (closed squares) and calculation including real (dashed line), virtual (dash-dotted line), and both virtual and real (solid line) transitions. The dotted line exhibits the temperature dependence of the population relaxation.

periment. We also present the temperature dependence of the polaron linewidth due to virtual acoustic phonon scattering (dash-dotted line), and the calculated contribution to the polaron linewidth due to real transitions $N(\Delta_{pp})\Gamma_{pp}(\Delta_{pp})$ (dashed line). Contributions of real and virtual transitions to the dephasing are comparable up to 60 K. However, for higher temperatures, the virtual contribution becomes dominant as it is enhanced quadratically with temperature. The measured and calculated homogeneous linewidths Γ_2 increase rapidly from $\approx 15 \mu\text{eV}$ up to $\approx 150 \mu\text{eV}$ with increasing temperature from 10 to 120 K. This behavior contrasts with the weak temperature dependence of the polaron population relaxation to the ground state Γ_1 over the same temperature range [dotted line in Fig. 4(d)], indicating that the dephasing is dominated by pure dephasing for higher temperatures.

In summary, these FWM studies of intersublevel dephas-

ing in *n*-doped quantum dots reveal oscillatory behavior of the polarization decay for times < 5 ps after excitation, followed by a single exponential decay yielding dephasing times of 90 ps at 10 K. The oscillation at short times arises from coherent acoustic phonon generation due to resonant excitation of both the zero phonon line and the peaked acoustic phonon sidebands associated with the intersublevel transition. Our results provide fresh insight into decoherence mechanisms of electron states in QDs.

Funding was provided by the UK Engineering and Physical Sciences Research Council (EPSRC) under the EPSRC/FOM agreement, and Grants No. GR/S76076/01 and No. GR/T21158/01. The LPA (UMR 8551) is associated with the CNRS and the Universities Paris 6 and Paris 7. In addition, we would like to thank B. Redlich and the FELIX staff for their help and guidance.

- ¹P. Borri, W. Langbein, S. Schneider, U. Woggon, R. L. Sellin, D. Ouyang, and D. Bimberg, *Phys. Rev. Lett.* **87**, 157401 (2001).
- ²D. Birkedal, K. Leosson, and J. M. Hvam, *Phys. Rev. Lett.* **87**, 227401 (2001).
- ³J. R. Petta, A. C. Johnson, J. M. Taylor, E. A. Laird, A. Yacoby, M. D. Lukin, C. M. Marcus, M. P. Hanson, and A. C. Gossard, *Science* **309**, 2180 (2005).
- ⁴A. Greilich, D. R. Yakovlev, A. Shabaev, Al. L. Efros, I. A. Yugova, R. Oulton, V. Stavarache, D. Reuter, A. Wieck, and M. Bayer, *Science* **313**, 341 (2006).
- ⁵S. Sauvage, P. Boucaud, T. Brunhes, M. Broquier, C. Crépin, J.-M. Ortega, and J.-M. Gérard, *Phys. Rev. B* **66**, 153312 (2002).
- ⁶S. Hameau, Y. Guldner, O. Verzellen, R. Ferreira, G. Bastard, J. Zeman, A. Lemaître, and J. M. Gérard, *Phys. Rev. Lett.* **83**, 4152 (1999).
- ⁷S. Sauvage, P. Boucaud, R. P. S. M. Lobo, F. Bras, G. Fishman, R. Prazeres, F. Glotin, J. M. Ortega, and J. M. Gerard, *Phys. Rev. Lett.* **88**, 177402 (2002).
- ⁸E. A. Zibik, L. R. Wilson, R. P. Green, G. Bastard, R. Ferreira, P. J. Phillips, D. A. Carder, J.-P. R. Wells, J. W. Cockburn, M. S. Skolnick, M. J. Steer, and M. Hopkinson, *Phys. Rev. B* **70**, 161305(R) (2004).
- ⁹L. Besombes, K. Kheng, L. Marsal, and H. Mariette, *Phys. Rev. B* **63**, 155307 (2001); I. Favero, G. Cassabois, R. Ferreira, D. Darsion, C. Voisin, J. Tignon, C. Delalande, G. Bastard, Ph. Rousignol, and J. M. Gérard, *Phys. Rev. B* **68**, 233301 (2003).
- ¹⁰Y. Toyozawa, *Optical Processes in Solids* (Cambridge University Press, Cambridge, 2003).
- ¹¹R. A. Kaindl, S. Lutgen, M. Woerner, T. Elsaesser, B. Nottelmann, V. M. Axt, T. Kuhn, A. Hase, and H. Künnel, *Phys. Rev. Lett.* **80**, 3575 (1998); R. A. Kaindl, K. Reimann, M. Woerner, T. Elsaesser, R. Hey, and K. H. Ploog, *Phys. Rev. B* **63**, 161308(R) (2001).
- ¹²S. Sauvage and P. Boucaud, *Appl. Phys. Lett.* **88**, 063106 (2006).
- ¹³M. S. Sherwin, A. Imamoglu, and T. Montroy, *Phys. Rev. A* **60**, 3508 (1999); B. E. Cole, J. B. Williams, B. T. King, M. S. Sherwin, and C. R. Stanley, *Nature (London)* **410**, 60 (2001).
- ¹⁴B. A. Carpenter, E. A. Zibik, M. L. Sadowski, L. R. Wilson, D. M. Whittaker, J. W. Cockburn, M. S. Skolnick, M. Potemski, M. J. Steer, and M. Hopkinson, *Phys. Rev. B* **74**, 161302(R) (2006).
- ¹⁵O. Stier, M. Grundmann, and D. Bimberg, *Phys. Rev. B* **59**, 5688 (1999).
- ¹⁶G. Bester, A. Zunger, X. Wu, and D. Vanderbilt, *Phys. Rev. B* **74**, 081305(R) (2006).
- ¹⁷G. Bester and A. Zunger, *Phys. Rev. B* **71**, 045318 (2005).
- ¹⁸D. Zimdars, A. Tokmakoff, S. Chen, S. R. Greenfield, M. D. Fayer, T. I. Smith, and H. A. Schwettman, *Phys. Rev. Lett.* **70**, 2718 (1993).
- ¹⁹This power is significantly lower compared with the excitation power of $\sim 7 \text{ kW/mm}^2$ used in Ref. 11 for FWM measurements in the case of intersubband transitions in QWs.
- ²⁰See, for example, J. Shah, *Ultrafast Spectroscopy of Semiconductors and Semiconductor Nanostructures* (Springer, New York, 1999).
- ²¹X.-Q. Li, H. Nakayama, and Y. Arakawa, *Phys. Rev. B* **59**, 5069 (1999).
- ²²As the population decay of the p_x state is bi-exponential, we refer to T_1 as the population decay at long delay times (as measured in Ref. 8), i.e., after the partial population decay due to thermalization with the p_y state.
- ²³For this measurement another QD sample with absorption peak maximum at $\sim 48 \text{ meV}$ was studied.
- ²⁴I. Vurgaftman, J. R. Meyer, and L. R. Ram-Mohan, *J. Appl. Phys.* **89**, 5815 (2001).
- ²⁵G. D. Mahan, *Many-Particle Physics* (Kluwer, New York, 2000).
- ²⁶The dot parameters we used in our calculations are the same as in T. Grange *et al.*, *New J. Phys.* **9**, 259 (2007).
- ²⁷E. A. Muljarov and R. Zimmermann, *Phys. Rev. Lett.* **93**, 237401 (2004); E. A. Muljarov, T. Takagahara, and R. Zimmermann, *ibid.* **95**, 177405 (2005).
- ²⁸T. Grange, R. Ferreira, and G. Bastard (unpublished).
- ²⁹A. Vagov, V. M. Axt, and T. Kuhn, *Phys. Rev. B* **67**, 115338 (2003).
- ³⁰However, the contribution of this initial polaron decoherence is smaller compared to the excitonic case: the weight of the ZPL decreases from $Z=0.98$ at 0 K to $Z=0.77$ at 100 K, while at the same temperature $Z\sim 0.3$ for excitonic transitions; see P. Borri, W. Langbein, U. Woggon, V. Stavarache, D. Reuter, and A. D. Wieck, *Phys. Rev. B* **71**, 115328 (2005).